



Equifrequency curve dispersion in dielectric-loaded plasmonic crystals

C. J. Regan, L. Grave de Peralta, and A. A. Bernussi

Citation: *J. Appl. Phys.* **111**, 073105 (2012); doi: 10.1063/1.3702790

View online: <http://dx.doi.org/10.1063/1.3702790>

View Table of Contents: <http://jap.aip.org/resource/1/JAPIAU/v111/i7>

Published by the [American Institute of Physics](#).

Related Articles

Surface plasmon on topological insulator/dielectric interface enhanced ZnO ultraviolet photoluminescence
AIP Advances **2**, 022105 (2012)

Optical coupling of surface plasmons between graphene sheets
Appl. Phys. Lett. **100**, 131111 (2012)

Tuning asymmetry parameter of Fano resonance of spoof surface plasmons by modes coupling
Appl. Phys. Lett. **100**, 131110 (2012)

Resonant surface magnetoplasmons in two-dimensional magnetoplasmonic crystals excited in Faraday configuration
J. Appl. Phys. **111**, 07A946 (2012)

Robust exciton-polariton effect in a ZnO whispering gallery microcavity at high temperature
Appl. Phys. Lett. **100**, 101912 (2012)

Additional information on *J. Appl. Phys.*

Journal Homepage: <http://jap.aip.org/>

Journal Information: http://jap.aip.org/about/about_the_journal

Top downloads: http://jap.aip.org/features/most_downloaded

Information for Authors: <http://jap.aip.org/authors>

ADVERTISEMENT

**FIND THE NEEDLE IN THE
HIRING HAYSTACK**

Post jobs and reach
thousands of hard-to-find
scientists with specific skills

<http://careers.physicstoday.org/post.cfm> **physicstoday JOBS**

Equipfrequency curve dispersion in dielectric-loaded plasmonic crystals

C. J. Regan,^{1,2} L. Grave de Peralta,^{2,3} and A. A. Bernussi^{1,2,a)}

¹Department of Electrical and Computer Engineering, Texas Tech University, Lubbock, Texas 79409, USA

²Nano Tech Center, Texas Tech University, Lubbock, Texas 79409, USA

³Department of Physics, Texas Tech University, Lubbock, Texas 79409, USA

(Received 28 December 2011; accepted 2 March 2012; published online 10 April 2012)

We present a quantitative description of the momentum-space dispersion and directivity of light propagation in dielectric-loaded plasmonic crystals. In our analysis the three-dimensional lossy plasmonic crystals are modeled by two-dimensional lossless dielectric crystals with real effective refractive indexes. Simulated equipfrequency curves are in excellent agreement with measured Fourier plane images obtained from dye-doped dielectric-loaded plasmonic crystals with different lattice geometries and parameters. Our results provide fundamental information about the origin of the directional bandgaps in these structures. © 2012 American Institute of Physics. [<http://dx.doi.org/10.1063/1.3702790>]

I. INTRODUCTION

Surface plasmon polaritons (SPP), or plasmonics, is one of the most recently investigated topics in modern optics research due to its unique capability of guiding and confining light in spatial regions far below the ones predicted by the classical diffraction limit of the light.¹ Specifically, plasmonic crystals (PmC) are the key building block in a variety of newly developed micron- and nanoscale photonic devices designed for different applications such as resonant cavities, waveguides, multiplexers, splitters, and for dispersion engineering, sensing, and ultrahigh resolution imaging.^{2–4} Among the various investigated configurations, dielectric-loaded PmC are particularly attractive due to their relatively simple realization, strong light confinement within the subwavelength dielectric layer, and the possibility of propagation loss reduction, or even compensation, when the dielectric layer is doped with an active gain medium.⁵ Consequently, detailed experimental characterization and simulation analysis of dielectric-loaded PmC are fundamental to evaluate and to predict the performance of such structures for different photonic applications.

There have been recent reports of experimental results on the characterization of dye-doped dielectric-loaded PmC using plasmon-coupled leakage radiation.^{6,7} Although clear evidence of photonic Fermi surfaces and the presence of directional gaps were verified experimentally, the design of PmC continues to be purely empirical. In order to provide support design for specific device application and to obtain quantitative information concerning the bandgap formation in PmC, simulations of these structures are of critical importance. Simulations of different types of PmC have been previously reported.^{8–13} However, these simulations are quite often challenging due to the inherent presence of the dispersive and lossy metal layer. In contrast, simulations of dielectric photonic crystal (PC) counterparts are usually performed using the plane wave expansion (PWE) method,¹⁴ whereby Maxwell's equations are formulated as an eigenvalue prob-

lem with periodic boundary conditions. This approach however cannot be directly extended to PmC, since the dielectric tensor is no longer Hermitian.² This has led to the use of alternative sophisticated and time consuming approaches to evaluate the band structure of crystals in dispersive media.^{8–13} The problem becomes even more complex as one attempts to calculate the behavior of a three-dimensional (3D) structure with two-dimensional (2D) periodicity. This is the case of typical dielectric-loaded PmC where, for instance, holes are present in the dielectric layer but not in the metal layer. Consequently a 3D problem must be solved, as opposed to that one where a 2D approximation can be employed for the case of holes in a metal sheet.⁸

In this work we present a quantitative analysis of the equipfrequency dispersion curves of dye-doped dielectric-loaded PmC.⁶ In our approach the 3D PmC can be approximated by a 2D periodic structure with appropriate real effective refractive indexes. As a result, the PWE method can be then used to predict the band structure of 3D PmC. In order to validate the proposed method we compare the simulated results with those obtained from SPP-tomography measurements on dielectric loaded plasmonic crystals with different lattice geometries and dimensions.⁶ Excellent agreement between simulated and measured equipfrequency dispersion curves in the momentum (k) space was verified for all plasmonic crystals investigated here. In addition, we present a qualitative analysis concerning the intensity contrast observed in the momentum-space images of the PmC and which effectively provides direct information on the directivity of the light propagating within the crystals. To the best of our knowledge, this is the first time that a detailed comparison between simulated equipfrequency dispersion curves and measured Fourier Plane (FP) images from dielectric-loaded PmC is presented.

II. EFFECTIVE INDEX AND PLANE WAVE EXPANSION APPROACH

Schematic illustrations of a dielectric-loaded plasmonic crystal with square lattice symmetry are shown in Figs. 1(a)

^{a)}Author to whom correspondence should be addressed. Electronic mail: arylon.bernussi@ttu.edu.

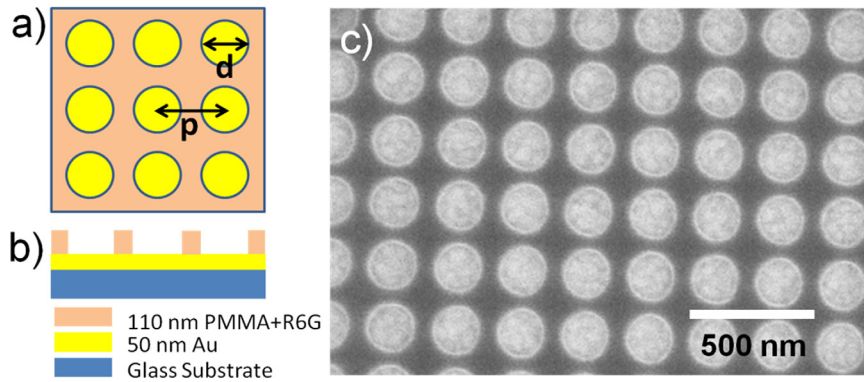


FIG. 1. Illustration of a plasmonic crystal with rectangular lattice symmetry (a) top view, (b) cross-section view (b), and (c) SEM image of a fabricated square lattice plasmonic crystal sample with $d = 200$ nm and $p = 300$ nm.

and 1(b). The samples consist of a glass substrate, a thin gold film and a patterned PMMA (polymethylmethacrylate) layer. We assume that the structure can be modeled by a simple 2D PC with two distinct real effective refractive indexes: n_1 corresponding to the metal-PMMA region and n_2 to the metal-air region. Under this assumption the band structure of the plasmonic crystal can be then determined using the PWE method applied to an equivalent PC with the real parts of the effective refractive indexes n_1 and n_2 . We justify this assumption as follows: while the PmC is highly lossy, we can suppose real effective refractive indexes as a good approximation for the eigenmode solution of the 3D PmC since the real part of the wavevector depends solely on the real part of the refractive index. This can be understood using the following relation:

$$k = k' + ik'' = \frac{2\pi n}{\lambda_0} = \frac{2\pi}{\lambda_0} (n' + in''), \quad (1)$$

where n is the complex effective refractive index and k is the complex wavevector of the guided plasmon mode. By equating real and imaginary parts of (1) we verify that k' , the real part of the wavevector depends only on n' , the real part of the effective refractive index of the mode. The shape of the equifrequency lines in the FP images of the PmC represents the real part of k (k'), while their line widths are related to the imaginary part of k (k'') which in turn is proportional to the reciprocal of the propagation length of the guided plasmon mode.⁵ This suggests that the shape of the equifrequency lines in the momentum space depends primarily on the real part of the effective refractive index of the PmC. In other words, the shape of the equifrequency lines should not be altered when only real effective indexes are considered. In addition, we also can consider a 2D crystal geometry to first approximation due to the extremely high confinement of the electromagnetic field near the metal layer. If the values of k'' are known, then one can, in principle, also model the intensity of the equifrequency lines observed in the FP images of dielectric-loaded PmC by adding the finite line widths corresponding to the plasmon propagation length.

In order to verify the effectiveness of our approach to simulate the equifrequency lines of the PmC, the effective refractive indexes n_1 and n_2 must be first determined. We used finite element method (FEM) analysis to determine the effective indexes of the fundamental plasmon mode.

Material refractive indexes¹⁵ and thicknesses (t) used in our simulations were: (a) gold layer: $n_{\text{Au}} = 0.30 + i2.59$ and $t_{\text{Au}} = 50$ nm; (b) PMMA layer: $n_{\text{PMMA}} = 1.49$ and $t_{\text{PMMA}} = 110$ nm. Simulations were carried out for the free space wavelength $\lambda_0 = 568$ nm. We assume a wide cross-sectional computational window region ($> 10 \mu\text{m}$) and an air superstrate layer of $10 \mu\text{m}$. The glass substrate ($n = 1.52$) was also included in our simulations. Using the above parameters and geometry we determined the real part of the effective refractive indexes as: $n_1 = 1.014$ and $n_2 = 1.075$.

Using n_1 and n_2 from the FEM analysis we calculated the entire band surface of the crystal over the full range of k -space using the PWE method, rather than only along the high crystal symmetry lines. By slicing this surface at the frequency of interest ($\lambda_0 = 568$ nm) we obtained the desired equifrequency contour lines. Band structure simulations were performed using BandsolveTM from RSoft.¹⁶ In our approach we used the periodic zone scheme as opposed to the typically used reduced scheme [plotting the band solutions only within the first Brillouin zone (FBZ)]. This allows us to perform a direct comparison between simulated and experimental equifrequency curves as some of our experimental data lies outside of the FBZ.

III. EXPERIMENT

Details of sample fabrication and the SPP tomography technique can be found in Refs. 6 and 17. The schematics and a scanning electron microscope (SEM) image of a fabricated plasmonic crystal with square lattice symmetry are shown in Fig. 1. Plasmonic crystals investigated here consist of periodic arrays of air holes defined on 110 nm thick dye-doped (Rhodamine 6 G) PMMA layer, with peak emission at ~ 568 nm wavelength, using electron-beam lithography technique. The dye-doped dielectric layer was spun over a 50 nm thick gold film deposited on a glass substrate. The dye molecules were excited by a 532 nm wavelength pumping laser. The excited molecules emit randomly, and a fraction of the emitted light couples evanescently to the allowed surface plasmon modes.¹⁸ For a uniform PMMA layer, this corresponds to light emission in all directions, but the presence of the crystal will alter how the photons are allowed to propagate within the crystal.⁶ By collecting the leaked light from the sample and transforming the image into the FP with a high numerical aperture (NA) microscope objective lens, one

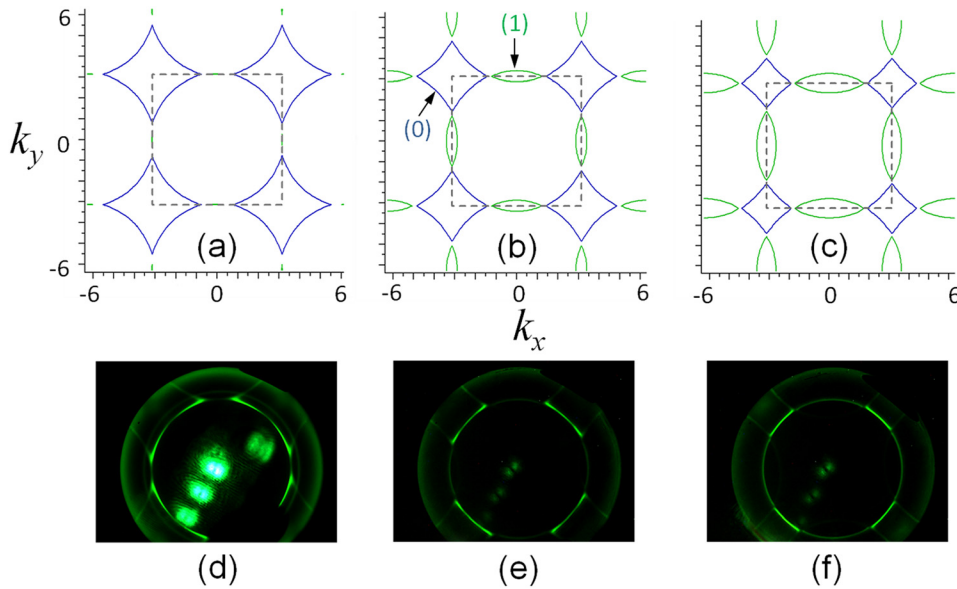


FIG. 2. Simulated (a)–(c) equifrequency curves for square symmetry plasmonic crystals using the PWE method using $n_1=1.014$ and $n_2=1.075$. Blue lines represent points in the lowest band 0, and green in band 1. The FBZ is shown in dashed gray for each figure. Measured (d)–(e) equifrequency curves for square symmetry dielectric loaded plasmonic crystals consisting of holes in the PMMA above the gold layer. For all crystals d is kept constant at 200 nm for (a) and (d), $p=280$ nm for (b) and (e), and $p=320$ nm for (c) and (f).

obtains the corresponding momentum-map of the photons propagating in the crystal.⁶ Bright intensity in the equifrequency contour lines corresponds to an allowed propagating mode. The light intensity at each point in the k -space is proportional to the density of optical states (DOS) at that point. For instance, in the image regions where Bragg diffraction occurs at the crossings of Brillouin zone boundaries, the DOS is zero, and this corresponds to dark regions of the FP image.

The signature of surface plasmon propagation in the FP of a uniform dye-doped dielectric layer over a metal film consists of a bright continuous ring with radius proportional to the guided mode effective refractive index and width proportional to the mode propagation losses. There is also a weak background of light which corresponds to the maximum angle collected by the microscope, and therefore is related to the NA of the collecting microscope objective

lens. For dielectric loaded plasmonic crystals,⁶ extra rings centered at the reciprocal lattice points of the crystal, similar to a Harrison construction in solid-state physics,¹⁹ are observed since the Bloch function is periodic in the momentum space with periodicity G , the reciprocal lattice vectors of the crystal.

Shown below are simulated and measured equifrequency curves for PmC with square (Fig. 2) and hexagonal (Fig. 3) lattice symmetries for three different periods. An excellent agreement between the proposed simulation approach and the experiments are evident in those two sets of figures for all plasmonic crystals investigated here. The simulated equifrequency curves shown in Figs. 2(a)–2(c) and Figs. 3(a)–3(c) were obtained using n_1 and n_2 determined from the FEM analysis, hole diameter of $d=200$ nm, and varying *only* the period (p) of the crystal lattice. The FBZs are also shown for clarification purposes. The simulated equifrequency curves

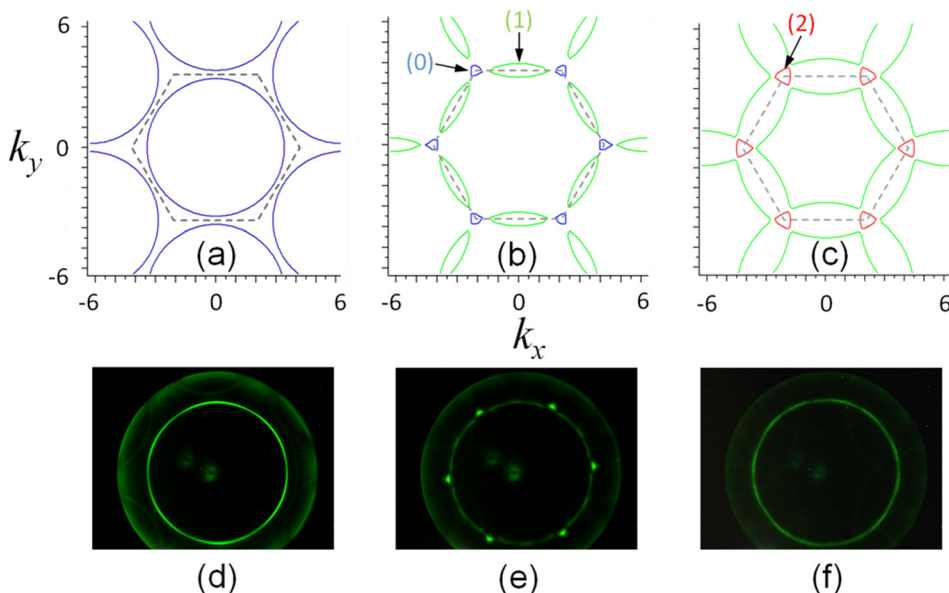


FIG. 3. Simulated (a)–(c) equifrequency curves for hexagonal symmetry plasmonic crystals using the PWE method using $n_1=1.014$ and $n_2=1.075$. Blue lines represent points in the lowest band 0, green in band 1, and red in band 2. The FBZ is shown in dashed gray for each figure. Measured (d)–(e) equifrequency curves for hexagonal symmetry dielectric loaded plasmonic crystals consisting of holes in PMMA above gold. For all crystals d is kept constant at 200 nm and $p=300$ nm for (a) and (d), $p=350$ nm for (b) and (e), and $p=400$ nm for (c) and (f).

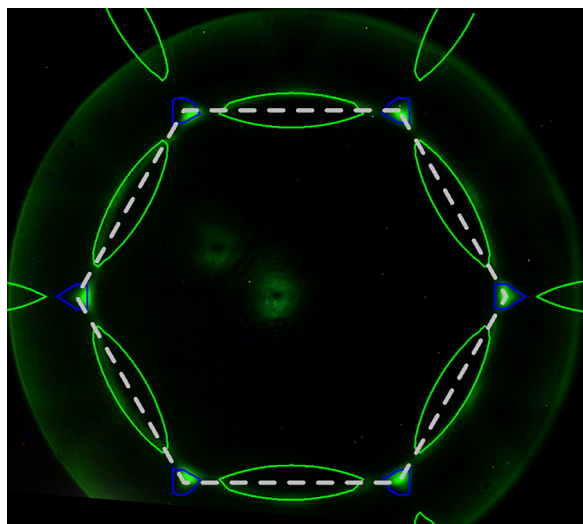


FIG. 4. Overlay of Fig. 3(b) on the top of Fig. 3(e) demonstrating the effectiveness of our method.

[Figs. 2(a)–2(c)] are typical for square lattice photonic crystals outside of the bandgap region.^{2,20} As can be observed from those figures there are several diffraction orders of the equifrequency lines with gaps taking place at Brillouin zone crossings where Bragg diffraction occurs. However, rather than plotting a single band for multiple frequencies to investigate how the dispersion changes, as is often performed in the simulations of dielectric photonic crystals, we plot multiple bands for a singular frequency. This analysis is particularly useful when investigating k -values which lie outside the FBZ. This is because any part of the central ring which exists in the Brillouin zone of j th order must also exist in the corresponding indexed band number j .¹⁹ For the plots shown in Fig. 2, k is normalized to the period ($p = 1$).

In order to provide convincing evidence of the effectiveness of the proposed simulation approximation method we show in Fig. 4 the overlay of simulated [Fig. 3(b)] and experimental [Fig. 3(e)] equifrequency curves for the plasmonic crystal with hexagonal lattice, $d = 200$ nm and $p = 350$ nm. It is evident from Fig. 4 the excellent agreement between simulated and experimental curves. Similar excellent matching was observed for the other plasmonic samples investigated here.

IV. RESULTS AND DISCUSSION

The results shown in Figs. 2–4 demonstrate unambiguously that the directional bandgaps and equifrequency contours of a rather complex dielectric-loaded PmC can be predicted using the real effective refractive index approach. However, the simulation does not predict the changes in the relative intensity of different equifrequency contours in the FP images, since the PWE method provides information about the allowed propagating modes and not the DOS. Therefore, we can obtain additional qualitative, but very useful, information about the directivity of light propagation within the plasmonic crystals by plotting multiple bands. From a direct comparison between the FP images

and the equifrequency curves, it is clear that the light tends to concentrate in the lowest order available band. This is the case when bands 0 and 1 are present and the line intensity contrast is large (see Fig. 4). This argument is also valid for bands 1 and 2, where the line intensity contrast is smaller [as can be seen in Fig. 3(f)]. This is not surprising considering that the equifrequency curves intersects the FBZ at the crossing between bands 0 and 1 but intersects the second Brillouin zone (SBZ) at the crossing between bands 1 and 2, which is therefore a higher order effect. As we can see in Fig. 3(d), it is also evident that the optical DOS is higher where the ring is closer to the FBZ boundary. This is supported by simulation results on photonic crystals where the calculated DOS has a maximum at the band-edge and always occurs at a high symmetry point lying on the FBZ boundary.²

It should be pointed out here that the simulations of the equifrequency dispersion curves in PmC have limitations. For example, the frequency dispersion and ohmic losses due to the presence of the metal layer (gold) were not taken into consideration in our analysis. The two effective indexes used in the simulations (PMMA-gold and air-gold) will change with the operating frequency, and this will alter slightly the equifrequency curves. The absence of losses in our simulations resulted in constant intensity equifrequency contours. The losses, for instance, can be determined experimentally from the width of a Lorentzian fit to spatial regions of the FP images of the PmC corresponding to different propagation directions. However, the excellent agreement between measured FP images and simulated equifrequency contours of dye-doped dielectric loaded PmC suggests that our approach is effective to predict light propagation in these structures and this is critical for future device design applications, such as super-prism and super-collimation. Another limitation of our analysis concerns in-plane propagation of modes in a two-dimensional slab waveguide. However, this is the predominant method for fabricating actual devices based on periodic structures and therefore warrants real application, as opposed to previous studies on infinitely long metal rods suspended in a dielectric.

V. CONCLUSIONS

In summary, we presented a simulation analysis of the equifrequency distribution in PmC using only the real part of the effective refractive indexes from distinct regions of the crystals. Our simulations were compared with measured FP images, obtained with the SPP tomography technique, on dye-doped dielectric-loaded PmC with square and hexagonal symmetries with different lattice periods. An excellent agreement between simulations and experiments was verified for all samples investigated here. Our analysis provides an effective tool for future device design based on dielectric-loaded PmC for different applications including super-collimation and super-prism. However, it should be noted from our experimental results that if the equifrequency lines crosses multiple bands, for a given frequency, the light will not be evenly distributed among the lines, which could cause a significant decrease in strength of the desired effect.

ACKNOWLEDGMENTS

This work was partially supported by the NSF CAREER Award (ECCS-0954490).

- ¹W. L. Barnes, A. Dereux, and T. W. Dereux, *Nature* **424**, 824 (2003).
- ²J. D. Joannopoulos, S. G. Johnson, J. N. Winn, and R. D. Meade, *Photonic Crystals: Molding the Flow of Light* (Princeton University Press, 2008).
- ³V. M. Malyarchuk, F. Hua, N. H. Mack, V. T. Velasquez, J. O. White, R. G. Nuzzo, and J. A. Rogers, *Opt. Express* **13**, 5669 (2005).
- ⁴A. Drezet, D. Koller, A. Hohenau, A. Leitner, F. R. Aussenegg, and J. R. Krenn, *Nano Lett.* **7**, 1697 (2007).
- ⁵J. Grandidier, G. C. de Francs, S. Massenot, A. Bouhelier, L. Markey, J. C. Weeber, C. Finot, and A. Dereux, *Nano Lett.* **9**, 2935 (2009).
- ⁶C. J. Regan, A. Krishnan, R. Lopez-Boada, L. Grave de Peralta, and A. A. Bernussi, *Appl. Phys. Lett.* **98**, 151113 (2011).
- ⁷D. G. Zhang, X. C. Yuan, and J. Teng, *Appl. Phys. Lett.* **97**, 231117 (2010).
- ⁸T. A. Kelf, Y. Sugawara, J. J. Baumberg, M. Abdelsalam, and P. N. Bartlett, *Phys. Rev. Lett.* **95**, 116802 (2005).
- ⁹K. Sakoda, N. Kawai, T. Ito, A. Chutinan, S. Noda, T. Mitsuyu, and K. Hirao, *Phys. Rev. B* **64**, 045116 (2001).
- ¹⁰E. Istrate, A. A. Green, and E. H. Sargent, *Phys. Rev. B* **71**, 195122 (2005).
- ¹¹A. J. Ward, J. B. Pendry, and W. J. Stewart, *J. Phys. Condens. Matter* **7**, 2217 (1995).
- ¹²Z. Y. Li and L. L. Lin, *Phys. Rev. E* **67**, 046607 (2003).
- ¹³S. Randhawa, M. U. Gonzalez, J. Renger, S. Enoch, and R. Quidant, *Opt. Express* **18**, 14496 (2010).
- ¹⁴S. G. Johnson and J. D. Joannopoulos, *Opt. Express* **8**, 173 (2001).
- ¹⁵L. G. Shulz, *J. Opt. Soc. Am.* **44**, 357 (1954).
- ¹⁶See <http://www.rsftdesign.com/for> simulation of equifrequency dispersion curves.
- ¹⁷S. P. Frisbie, C. F. Chesnutt, M. E. Holtz, A. Krishnan, L. Grave de Peralta, and A. A. Bernussi, *IEEE Photon. J.* **1**, 153 (2009).
- ¹⁸J. R. Lakowicz, *Anal. Biochem.* **324**, 153 (2004).
- ¹⁹W. A. Harrison, *Solid State Theory* (Dover, New York, 1980).
- ²⁰M. Notomi, *Phys. Rev. B* **62**, 10696 (2000).